

Article

Effect of Rolling Temperature and Subsequence Ageing on the Mechanical Properties and Microstructure Evolution of an Al-Cu-Li Alloy

Lin Wang ^{1,2}, Charlie Kong ³, Puneet Tandon ⁴, Alexander Pesin ^{5,*}, Denis Pustovoytov ⁵ and Hailiang Yu ^{1,2,*}

- ¹ State Key Laboratory of High Performance Complex Manufacturing, College of Mechanical and Electrical Engineering, Central South University, Changsha 410083, China; 153711078@csu.edu.cn
² Light Alloys Research Institute, Central South University, Changsha 410083, China
³ Mark Wainwright Analytical Centre, University of New South Wales, Sydney, NSW 2052, Australia; c.kong@unsw.edu.au
⁴ deLOGIC Lab, PDPM Indian Institute of Information Technology, Design and Manufacturing, Jabalpur 482005, Madhya Pradesh, India; ptandon@iiitdmj.ac.in
⁵ Laboratory of Mechanics of Gradient Nanomaterials, Novosibirsk State Technical University, 630090 Novosibirsk, Russia; pustovoytov_den@mail.ru
* Correspondence: pesin@bk.ru (A.P.); yuhailiang@csu.edu.cn (H.Y.)

Abstract: The mechanical properties and microstructure evolution of an Al-Cu-Li alloy sheet processed via hot rolling (HR) (at 400 °C and 500 °C) or cryorolling (CR) (at −100 °C and −190 °C) and subsequence aging at 160 °C for 10 h were investigated. Before aging, the highest ultimate tensile strength of 502 MPa was achieved when the sheets were cryorolled at −190 °C, while the better ultimate tensile strength of 476 MPa and the best elongation rate of 11.1% was achieved simultaneously when the sheets were cryorolled at −100 °C. The refined grains and numerous uniform deformation-induced dislocations microstructures were responsible for the improved strength and enhanced ductility of the cryorolled sheets compared to that of the alloy processed by hot rolling with a low dislocation density zone (LDDZ) and high dislocation density zone (HDDZ). After aging at 160 °C for 10 h, the ultimate tensile strength further improved resulted from the greater precipitation strengthening, and the increased precipitates provided greater resistance to dislocations movement resulting in the increased ductility although the dislocation density decreased. The uniform dislocation microstructures in the cryorolled sheets provide numerous nucleation sites for the precipitates, leading to higher strength after aging.



Citation: Wang, L.; Kong, C.; Tandon, P.; Pesin, A.; Pustovoytov, D.; Yu, H. Effect of Rolling Temperature and Subsequence Ageing on the Mechanical Properties and Microstructure Evolution of an Al-Cu-Li Alloy. *Metals* **2021**, *11*, 853. <https://doi.org/10.3390/met11060853>

Academic Editor: Elisabetta Gariboldi

Received: 26 April 2021

Accepted: 20 May 2021

Published: 22 May 2021

Keywords: Al-Cu-Li alloy; mechanical property; cryorolling; aging

Publisher's Note: MDPI stays neutral with regard to jurisdictional claims in published maps and institutional affiliations.



Copyright: © 2021 by the authors. Licensee MDPI, Basel, Switzerland. This article is an open access article distributed under the terms and conditions of the Creative Commons Attribution (CC BY) license (<https://creativecommons.org/licenses/by/4.0/>).

1. Introduction

Aluminum-copper-lithium (Al-Cu-Li) alloys have been widely used as structural materials for aerospace and aircraft vehicles [1–3]. A comprehensive review about the development of the third generation Al-Li alloy was reported by Rioja et al. [4] and quantitative calculations of the Al-Cu-Li alloy during the deformation process were operated [5]. The alloy is a typical precipitation strengthening alloy resulting from the T_1 (Al_2CuLi) or θ' (Al_2Cu) phases [6]. Zhou et al. studied the effects of creep aging parameters on mechanical properties and found that the yield strength and the ultimate tensile strength increased to 493 MPa and 540 Mpa, respectively, after being aged at 163 °C for 25 h [7]. With the increase of the Cu element, proper heat treatment can further improve the strength via increasing precipitation strengthening [8–10].

In the past 30 years, people have developed several severe plastic deformation (SPD) techniques to fabricate ultrafine-grained (UFG) materials, including high-pressure torsion [11], equal channel angular pressing [12], accumulative roll bonding (ARB) [13], and

asymmetric cryorolling (ACR) [14]. During these techniques, rolling has been widely used to fabricate UFG metallic sheets. Yu et al. [15] reported that the properties of the copper sheets subjected to ACR were better than that of the copper sheets subjected to asymmetric rolling because of the restriction of dislocation movement. Magalhães et al. investigated the mechanical properties and the microstructure evolution of AA6061 processed by conventional rolling, CR, asymmetric rolling, ACR before and after post-deformation heat treatments, respectively. They found that uniform elongation of the materials annealed after ACR increased, while the alloys' texture intensity reduced resulting from recovery and recrystallization phenomena [16]. During CR, refined grains and accumulated dislocations that resulted from the increased strain hardening were reasonable for the enhanced mechanical properties [17].

The deformation-induced dislocation microstructures could act as nucleation sites for precipitation, which can further improve the mechanical properties [18]. The excellent mechanical properties, the yield strength of 485 MPa, the ultimate tensile strength of 540 MPa, and the ductility of 11%, were achieved for an Al–Cu alloy through CR and subsequent aging [19]. Deng et al. reported that the mechanical properties of an Al–Cu–Li alloy could be improved significantly via CR followed by aging at 160 °C for 32 h [20]. Li et al. proposed that the temperature corresponding to peak hardness is negatively related to rolling reduction and is positively related to rolling temperature [21]. However, there are few reports about the mechanical properties and microstructure evolution of the Al–Cu–Li alloys processed by CR under different temperatures. When the rolling temperature was set as liquid nitrogen temperature, grains could be refined uniformly and the dislocation network formed. If the rolling temperature was set as a middle temperature during liquid nitrogen temperature and room temperature, the reports about the microstructure evolution were rare.

In this study, the mechanical properties and microstructure evolution of Al–Cu–Li alloy sheets fabricated by HR (at 400 °C and 500 °C) or CR (at –100 °C and –190 °C) and subsequent aging at 160 °C for 10 h were investigated.

2. Materials and Methods

The original materials were Al–Cu–Li alloy sheets with an initial size of 60 mm × 100 mm × 2 mm self-melted in the laboratory. The chemical composition listed in Table 1 has been confirmed by the Inductive Coupled Plasma-Optical Emission Spectroscopy (ICP-OES) test. The processing schedule was shown in Figure 1. The size of the tensile sample was shown in the lower-left corner of the figure. The alloy sheets were placed in the furnace at 500 °C for 1 h for homogenization. Rolling experiments were carried out on a multifunction 4-high rolling mill with a maximum rolling width of 300 mm and a work roll diameter of 80 mm. The rolling speed was set as 2 m/min. For each pass during CR or HR, the rolling reduction of each pass was 16% and the final thickness of the alloy sheet after six passes was about 0.7 mm. After HR or CR at different temperatures, the samples were air-cooled to room temperature. The rolling experiments were operated in a “dry friction” condition and the work rolls surfaces were smooth after being polished. Before each pass of rolling at 400 °C or 500 °C (HR 400 °C or HR 500 °C), the sheets were placed in the furnace for 3 min. Before each CR pass at –100 °C or –190 °C (CR –100 °C or CR –190 °C), the sheets were placed in the cryogenic furnace for >8 min. After rolling, the rolled sheets were aged at 160 °C for 10 h in an aging furnace.

Table 1. Chemical composition of Al–Cu–Li alloy.

Composition (Wt%)	Cu	Mg	Zn	Li	Ag	Mn	Zr	Al
Al–Cu–Li alloy	3.72	0.58	0.46	0.96	0.30	0.58	0.31	91.6

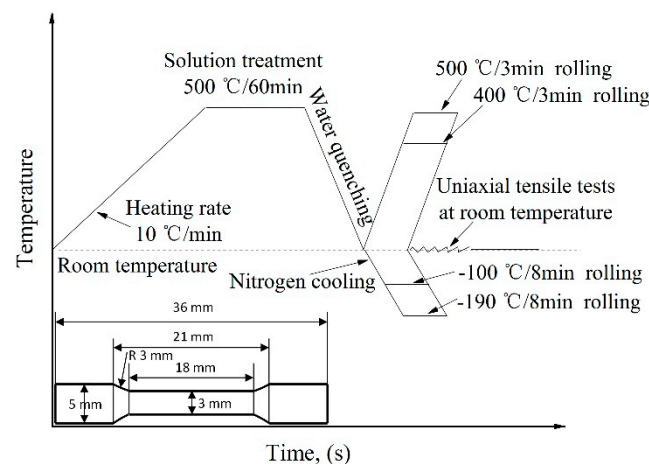


Figure 1. Processing schedule.

The tensile tests were carried out on an AGS-5/10 kN testing machine produced by Shimadzu Company (Suzhou, China) at a strain rate of 0.03 s^{-1} at room temperature. Each tensile test was repeated three times for the mean values to ensure accuracy. The fracture surface was examined utilizing the scanning electron microscopy (SEM) equipped on the platform of a Phenom Prox Desktop and the accelerating voltage was set as 15 kV. The morphology of grains after processing was studied using the optical microscope (the platform of VHX–5000) after the samples were etched with Keller’s reagent for about 16 s on the normal plane. A Philips CM200 transmission electron microscope, with a field-emission gun operating at 200 kV, was used to examine the cross-section microstructures in the rolling direction. A Thermo Fisher Helios G4 PFIB was used to prepare the transmission electron microscopy (TEM) specimens via the in situ lift-out technique. The range from 30° to 110° was detected by X-ray on a Bruker D8 Advance diffractometer. The step size was set as 0.02° and the Cu target was utilized in the diffraction test.

3. Results and Discussion

Figure 2 shows the mechanical properties of the Al–Cu–Li alloy sheets processed by rolling at different temperatures and subsequent aging at 160°C for 10 h. The ultimate tensile strength and the ductility of the alloy after rolling and aging were summarized in Figure 2b and Figure 2c,d respectively. After solution treatment at 500°C for 1 h, the ultimate tensile strength of 270 MPa and the elongation rate of 11.0% was obtained. When the Al–Cu–Li alloy was hot rolled at 400°C , the lowest ultimate tensile strength of 356 MPa and the lowest elongation of 8.1% was achieved. The ultimate tensile strength increased to 449 MPa for HR 500°C , to 476 MPa for CR -100°C and to 502 MPa for CR -190°C . The ductility increased to 9.5% for CR -190°C , to 10.7% for HR 500°C , to 11.1% for CR -100°C . The yield strength of the sheet processed by HR 400°C increased when the rolling temperature increased to 500°C and it further increased with the decreasing of the rolling temperatures. To elucidate the effects of rolling temperature on strain rate, the mechanism of dislocation movement and interaction was considered. More slip systems were easily activated during CR and the slip plane of screw dislocation changed to other planes which the Burgers vector b of the dislocation is common to. One possible origin of the screw dislocations pair was a thermal cross-slip of screw dislocations at different stress levels and the termination of the dipoles were edge dislocations [22]. The limit of dislocations multiplication increased when the alloy was subjected to CR in the temperature range. Additionally, the ultrafine grains with high dense dislocations deformed during CR facilitate the nucleation and growth of precipitates resulting from the lower activation energy barrier and increased free energy [23].

After aging at 160°C for 10 h, the ultimate tensile strength and the ductility increased and the ultimate tensile strength sequence was similar to that before aging. The highest ultimate tensile strength of 549 MPa and the elongation rate of 13.9% was achieved simul-

taneously when the sheets were processed by CR at $-190\text{ }^{\circ}\text{C}$ and subsequent aging for 10 h.

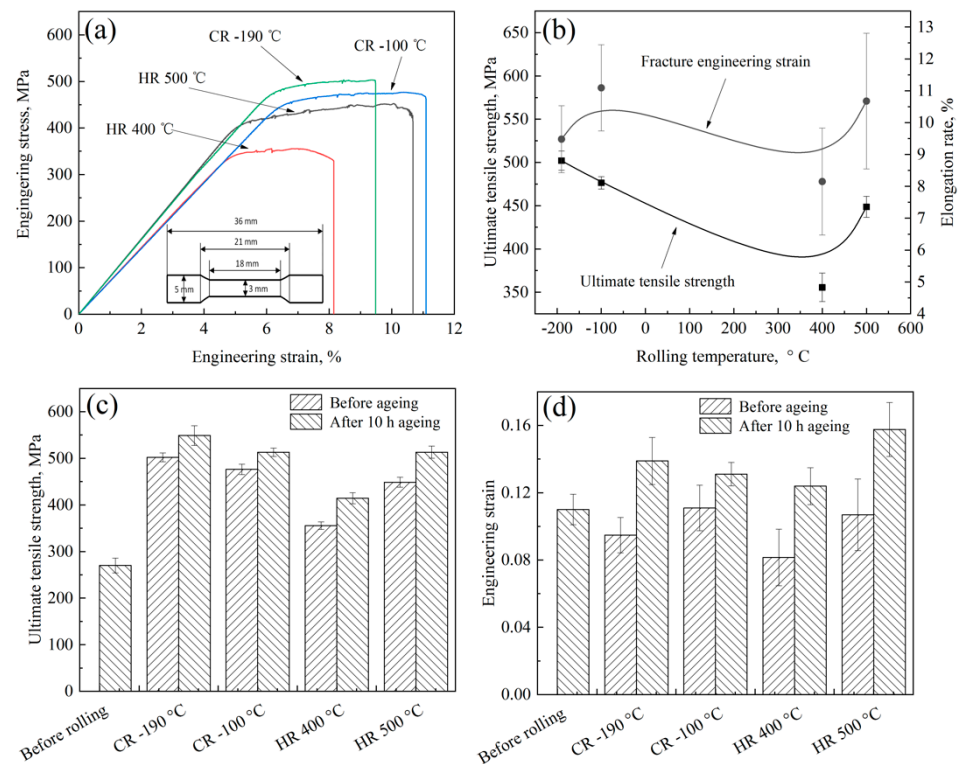


Figure 2. Mechanical properties of Al-Cu-Li alloy sheets after rolling and aging. (a) Engineering stress vs engineering strain curve of the Al-Cu-Li alloy sheets subjected to different processes; (b) Ultimate tensile stress and elongation vs rolling temperature; (c) Ultimate tensile stress vs rolling temperature after 10 h aging at $160\text{ }^{\circ}\text{C}$; (d) Engineering strain vs rolling temperature after aging at $160\text{ }^{\circ}\text{C}$ for 10 h.

Figure 3 shows the hardness's of the alloy sheets processed at different conditions. After solution treatment, the hardness of 118 HV was obtained. After rolling, the hardness increased due to the refined grains, increased dislocations, and precipitations. The highest hardness value of 148 HV was achieved when the alloy sheet was processed by CR at $-190\text{ }^{\circ}\text{C}$. After aging at $160\text{ }^{\circ}\text{C}$ for 10 h, it increased to 158 HV. The variation trend of hardness was similar to that of ultimate tensile strength.

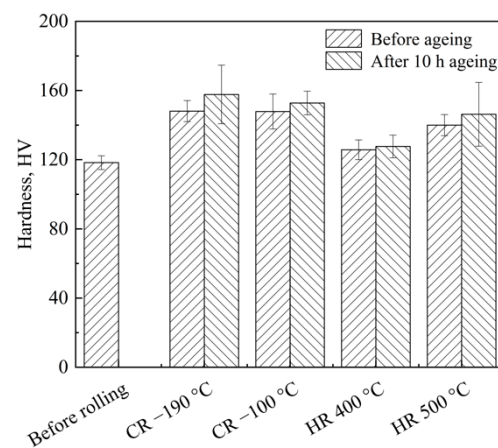


Figure 3. Hardness of Al-Cu-Li alloy sheets after rolling and aging.

Figure 4 shows optical microscopies of the Al-Cu-Li alloy by different processes. The grain size of the alloy after solution treatment was relatively large. After rolling, grains were refined to an elongated shape. With the decrease of rolling temperature, the mean grain size decreased obviously. After aging at 160 °C for 10 h, the grain size slightly increased and the sequence was similar to that before aging.

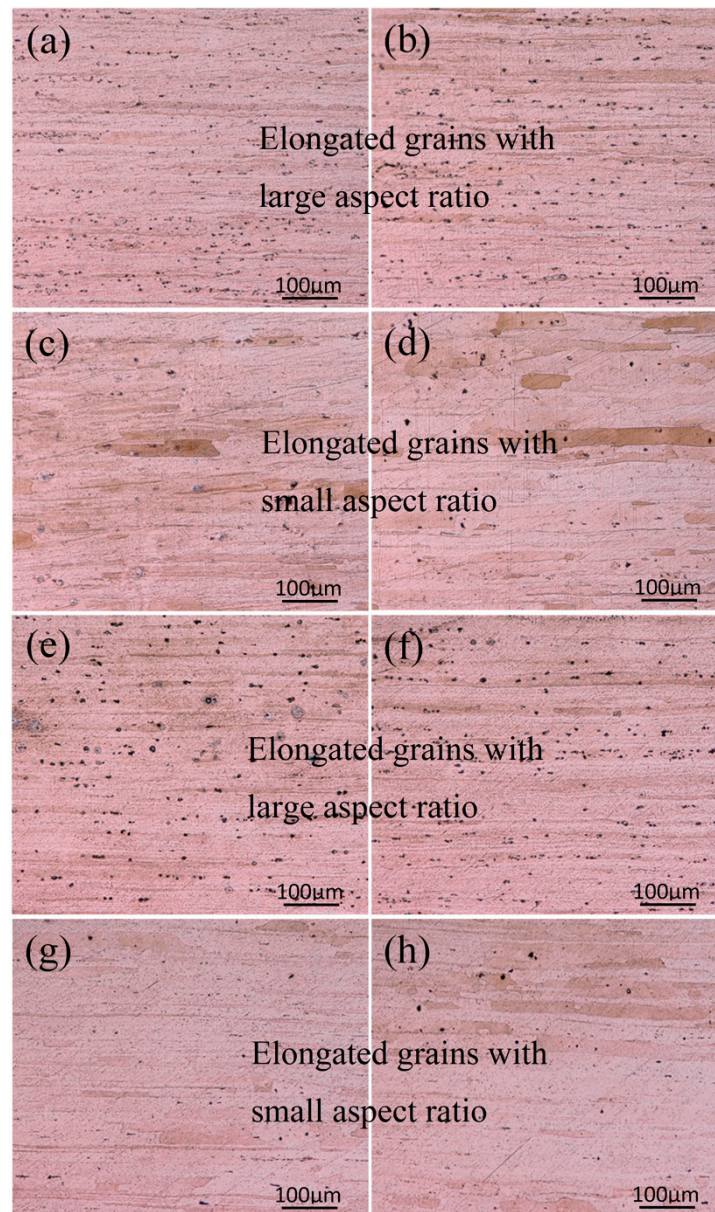


Figure 4. Optical microscopies of Al-Cu-Li alloys subjected to CR (at (a) $-190\text{ }^{\circ}\text{C}$ and (b) $-100\text{ }^{\circ}\text{C}$) and HR (at (c) $400\text{ }^{\circ}\text{C}$ and (d) $500\text{ }^{\circ}\text{C}$), as well as CR at (e) $-190\text{ }^{\circ}\text{C}$, and (f) $-100\text{ }^{\circ}\text{C}$, HR at (g) $400\text{ }^{\circ}\text{C}$, (h) $500\text{ }^{\circ}\text{C}$ and subsequent aging at $160\text{ }^{\circ}\text{C}$ for 10 h.

Figure 5 shows the TEM images of microstructures of sheets rolled at different temperatures. After rolling, numerous dislocation lines were formed and significantly entangled into dislocation clusters and into dislocation walls along grain boundaries and subgrain boundaries, which were marked by yellow lines and red lines. With the decrease of rolling temperature, more dislocations progressively accumulated and the dislocation debris, with a size of 80 nm, gradually moved to the dislocations cluster and dislocation walls entangled with them. Another great difference between the alloys processed by HR and CR was that the dislocation distribution in the cryorolled sample was relatively uniform while LDDZ

and HDDZ were obviously observed and they were distributed alternately, which have been marked in Figure 5c,d. When the low deformation strain was applied, vacancies and dislocations gradually formed and dislocations accumulated and entangled, forming dislocations clusters and dislocations walls with the increase of applied strain. As the hindering of the dislocation movement and the suppressing of the dynamic recovery, more dislocation networks were formed in the cryorolled samples. As the deformation strain further increased, the stress fields caused by dislocations started interacting with each other, leading to the relaxation and rearrangement of the dislocation network. The dislocation network gradually transformed into low angled dislocations cells, which were relatively thick and consisted of lesser geometrical necessary dislocation density. The dislocation cell boundaries prefer changing to subgrain boundaries leading to the formation of ultrafine subgrain microstructure in the alloy. Hence, a subgrain structure was observed in alloy processed by HR 500 °C and the microstructure free of dislocations was due to recovery phenomena at the relatively high temperature. HDDZ was observed because the dislocation cell boundaries were relatively stable compared to another dislocation network. Moreover, the second-phase particles have a certain pinning effect on the dislocation movement. A similar nonuniform dislocation structure was obtained when ferritic steel was pre-deformed at 25 °C by Tanaka et al. [24]. In addition to observing dislocations, the secondary-phase particles appeared beside the dislocation walls or dislocations clusters after HR, as shown in Figure 5c,d. With the increase of roll temperature, the fraction of the secondary-phase particles increased due to the larger nucleation energy.

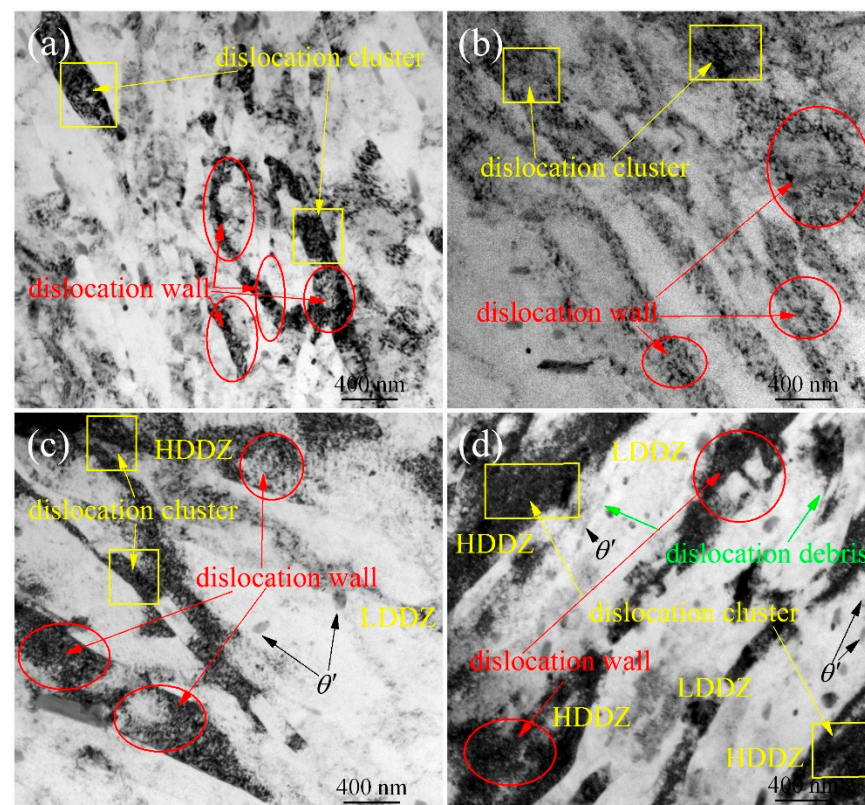


Figure 5. TEM images of Al-Cu-Li alloy subjected to CR at (a) -190 °C, and (b) -100 °C, HR at (c) 400 °C, (d) 500 °C.

Figure 6 shows the TEM images on a scale of 50 nm of the alloy subjected to CR -190 °C and HR 500 °C. With the reduction of 65%, numerous stack faults were formed in grains or at grain boundaries. When the alloy was processed by CR, the deformation-induced stack faults arranged along more than five directions while the two directions,

which have marked by black dotted lines, were observed in the alloy processed by HR 500 °C.

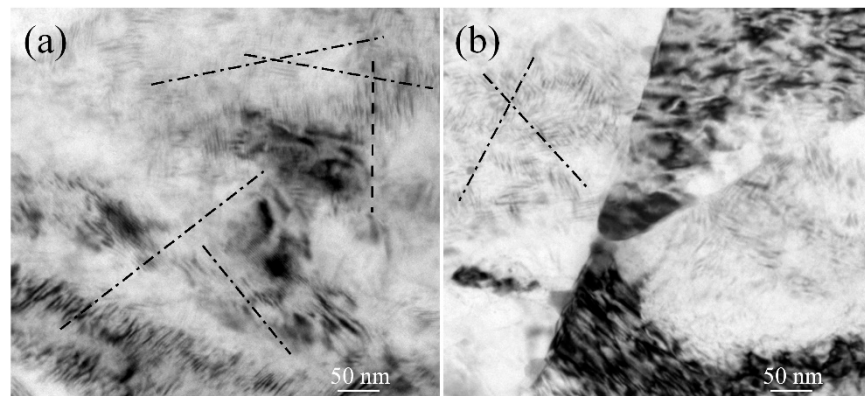


Figure 6. TEM images on a scale of 50 nm of Al-Cu-Li alloy subjected to (a) CR at -190 °C, and (b) HR at 500 °C.

Figure 7 shows TEM images of the samples after aging at 160 °C for 10 h. θ' was the main strengthening phase of the alloy. With the increase of the aging time, the secondary-phase particles gradually nucleated and grew while the dislocations decreased through annihilation. When the alloys were processed by CR -190 °C, the higher dislocation density in the alloy provided more nucleation sites for the precipitates leading to higher precipitation strengthening. While the rolling temperature increased from 400 °C to 500 °C, the diffusion energy of the solute atoms increased making it easy to precipitation. The number and area fraction of the secondary-phase particles in the samples rolled by CR or HR changes significantly.

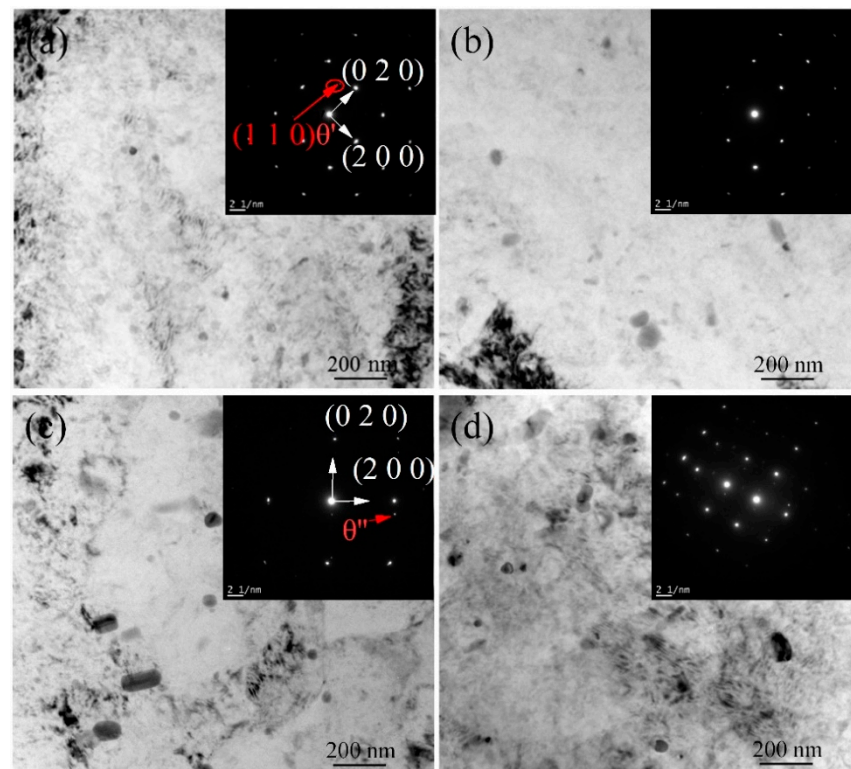


Figure 7. TEM images of the alloy subjected to CR at (a) 500 °C, and (b) 400 °C, HR at (c) -100 °C, (d) -190 °C after 10 h aging.

Figure 8 shows XRD patterns of the alloy processed by rolling at different temperatures and subsequent aging. The Williamson–Hall method was utilized to calculate the dislocation density [25]. The dislocation density and microstrain are shown in Figure 9. The highest dislocation density of $1.86 \times 10^{14} \text{ m}^{-2}$ was achieved when the alloy was processed by CR -190°C . With the increase of the rolling temperature, dislocation density decreased sharply. After aging at 160°C , dislocation density slightly decreased compared to the rolled samples at the corresponding temperature.

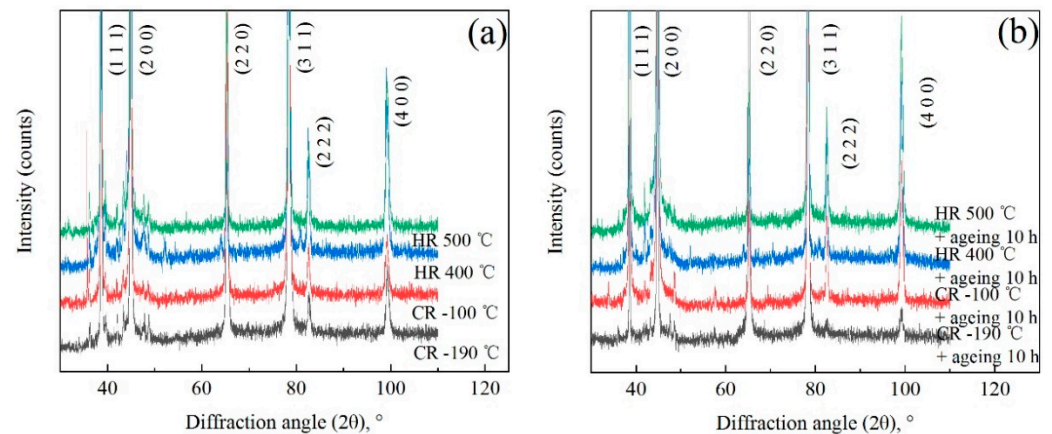


Figure 8. XRD patterns of the alloy subjected to (a) rolling (b) and subsequent aging at 160°C for 10 h.

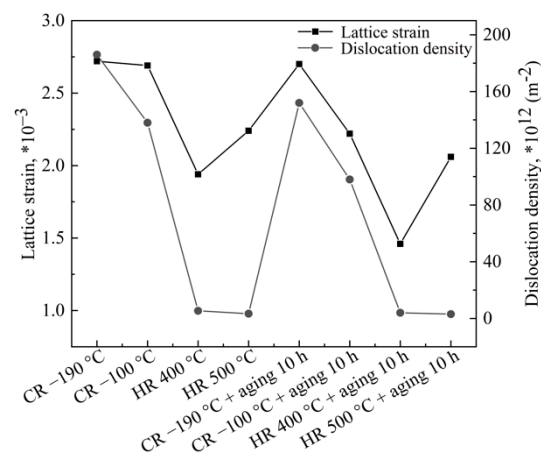


Figure 9. Lattice microstrain and dislocation density of the alloy processed under different conditions.

Figure 10 shows the fracture morphology of the Al–Cu–Li alloy sheets after rolling. The fracture mode is a mixture of ductile fracture and brittle fracture. The Al–Cu–Li alloy subjected to CR at -100°C and HR at 500°C show more dimples on the fracture which have been marked by yellow lines, and their ductility is good. However, for the Al–Cu–Li alloy sheets subjected to HR at 400°C , there are few shallow dimples. Moreover, there also are a few flat areas on the fracture surface that have been marked by red lines, and the ductility of the Al–Cu–Li alloy is the lowest.

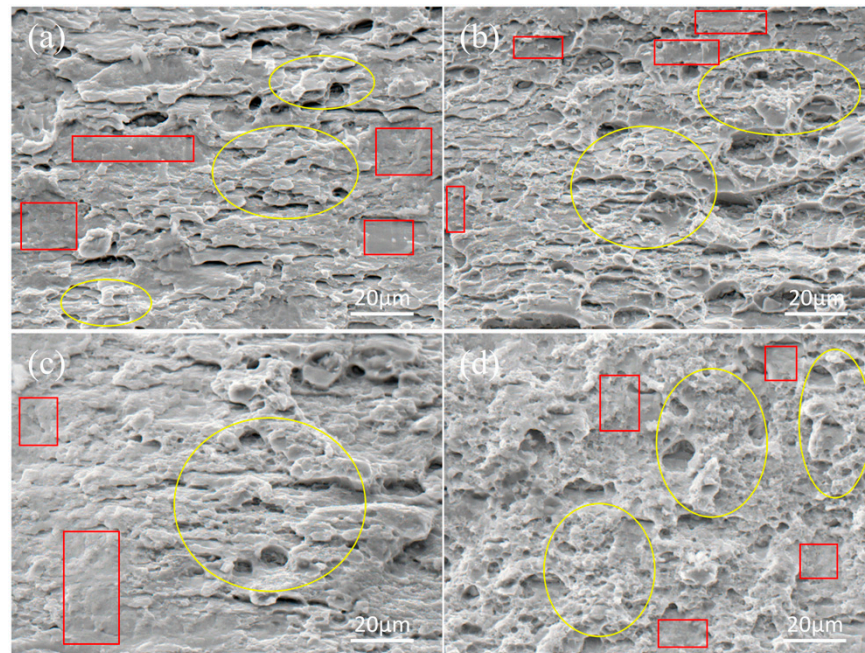


Figure 10. Fracture morphologies of the sheets subjected to CR at (a) $-190\text{ }^{\circ}\text{C}$ and (b) $-100\text{ }^{\circ}\text{C}$; HR at (c) $400\text{ }^{\circ}\text{C}$, (d) $500\text{ }^{\circ}\text{C}$.

Figure 11 shows fracture morphologies of the alloy rolled at different temperatures and subsequent aging at $160\text{ }^{\circ}\text{C}$ for 10 h. A comparison between Figures 10 and 11 shows that the dimples turned deeper and increased, which indicated the increase of the ductility of the sheets.

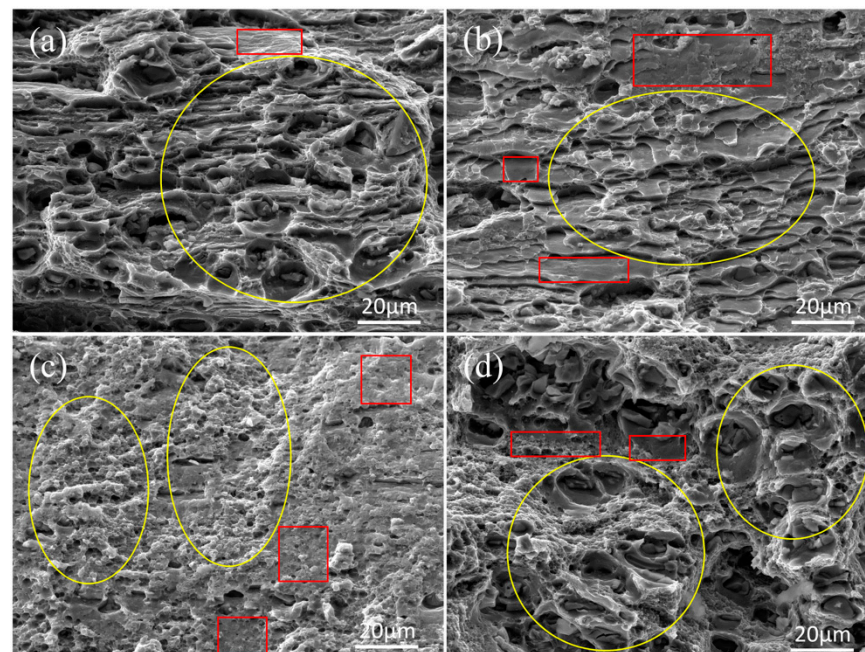


Figure 11. Fracture morphologies of the sheets subjected to CR at (a) $-190\text{ }^{\circ}\text{C}$, and (b) $-100\text{ }^{\circ}\text{C}$, HR at (c) $400\text{ }^{\circ}\text{C}$, (d) $500\text{ }^{\circ}\text{C}$ after 10 h aging.

From the above results, it is obvious that the rolling temperature plays a significant role in the fracture surface and mechanical properties of the Al-Cu-Li alloy sheets. It can be seen from Figure 2 that the differences of the ultimate tensile strength of 146.5 MPa are generated between the sheets processed by SR $400\text{ }^{\circ}\text{C}$ and SR $-190\text{ }^{\circ}\text{C}$. The grain sizes were

refined with the decreasing rolling temperature. The formation of small sized sub-grains appears during CR, which can be the reason for the increase of the ultimate tensile strength according to the Hall–Peach relationship [26]. In the processing of HR 500 °C, there are some clusters and a few amounts of precipitation, which can lead to better ultimate tensile strength compared with sheets processed by HR 400 °C. When the sheets were processed by CR, the driving energy of the dislocation movement was relatively low and dislocation movement and dynamic recovery were suppressed. Hence, new slip systems were active resulting in the appearance of more directions of stack fault arrangement compared with HR. When the rolling temperature increased from 400 °C to 500 °C, the size of the second-phase particles decreased and the number increased due to the higher solubility and a larger nucleation drive energy, which is shown in Figure 4, except the slight increase of the grain size. The fine second phase can hinder the movement of dislocations during tensile tests, resulting in enhanced strength and better ductility. Similar results have been obtained by Pathak et al. on the bulk ultrafine grain Al 2014 alloy. The percentage elongation of the alloy processed by CR + WR 170 °C (9.5%) was higher than that of the alloy processed by CR + WR 100 °C (4.5%) due to the formation of fine metastable spherical phase Al₂Cu and solid strengthening [27]. Interestingly, the CR processed sheets present better ductility than the sheets processed at 400 °C, resulting from the restrain of dynamic recovery and dislocation movement in the cryogenic temperature. Similar results have been reported in an Al-Mg alloy [28], high manganese steel [29], and CuZr alloy [30]. After aging at 160 °C for 10 h, the secondary-phase particle θ' and θ'' nucleated and grew, which has great strengthening effects. When the sheets were processed by CR at −190 °C and subsequent aging at 160 °C, the strengthening effects from refined grains, accumulated dislocations, precipitation were the biggest, leading to the highest strength.

4. Conclusions

The mechanical properties and microstructure evolution of an Al-Cu-Li alloy processed by CR and HR were investigated. The conclusions can be drawn as follows:

- (1) CR can significantly improve the tensile strength and ductility of Al-Cu-Li alloy sheets, the best ultimate tensile strength of 502 MPa was achieved for the specimens subjected to CR at −190 °C, and the best ductility of 11.1% was obtained for the specimens subjected to CR at −100 °C before aging. The highest ultimate tensile strength of 549 MPa and the elongation rate of 13.9% was achieved simultaneously when the sheets were processed by CR at −190 °C and subsequent aging for 10 h.
- (2) The mechanical properties of Al-Cu-Li alloy sheets are dependent on the grain sizes, precipitations and clusters, the dislocation microstructure, and the back stress distribution during rolling. Grains in cryorolled samples were seriously refined compared to that in the alloy processed by HR. Numerous deformation-induced dislocation networks were observed. HDDZ and LDDZ occurred in the hot-rolled samples, while it distributed uniformly with a more arranged direction in the cryorolled samples. After aging at 160 °C for 10 h, grains size slightly increased compared to that in the alloy rolled at the corresponding temperature. The deformation-induced dislocations can facilitate the nucleation and growth of the main strengthening phases θ' , which resulted in enhanced strength.

Author Contributions: Conceptualization, H.Y. and A.P.; methodology, L.W.; investigation, L.W., C.K., P.T., D.P.; resources, H.Y.; writing—original draft preparation, H.Y.; writing—review and editing, all authors; supervision, H.Y.; project administration, H.Y. and A.P.; funding acquisition, H.Y., and A.P. All authors have read and agreed to the published version of the manuscript.

Funding: This research was funded by the National Key Research and Development Program (Grant No.: 2019YFB2006500), National Natural Science Foundation of China (Grant number: 5167040503), Innovation Driven Program of Central South University (Grant No.: 2019CX006), the Science and Technology Innovation Program of Hunan Province (Grant No.: 2020RC2002), the Research Fund of the Key Laboratory of High Performance Complex Manufacturing at Central South University. A.P.

and D.P. appreciate the financial support of the research which was carried out within the framework of the implementation of the Resolution of the Government of the Russian Federation of April 9, 2010, No. 220 (Contract No. 075-15-2019-869 from May 12, 2019) and a grant from the Russian Science Foundation (project No. 20-69-46042 of 20.05.2020).

Institutional Review Board Statement: Not applicable.

Informed Consent Statement: Not applicable.

Data Availability Statement: The data presented in this study are available on request from the corresponding author.

Conflicts of Interest: The authors declare no conflict of interest.

References

- Triolo, A.; Lin, J.S.; Triolo, R. Early and late stages of demixing of a commercial Al-Li alloy. *J. Mater. Sci.* **2002**, *37*, 1207–1213. [[CrossRef](#)]
- Nazarov, S.A.; Ganiev, I.N.; Ganieva, N.I.; Calliari, I. Microstructure and mechanical properties of Al + 6%Li alloy containing rare-earth metals. *Vestnik Magnitogorskogo Gosudarstvennogo Tekhnicheskogo Universiteta im. G.I. Nosova. Vestn. Nosov Magnitogorsk State Tech. Univ.* **2017**, *15*, 63–68. [[CrossRef](#)]
- Nazarov, S.A.; Ganiev, I.N.; Norova, M.T.; Ganieva, N.I.; Calliari, I. Potentiodynamic study of the Al + 6% Li alloy doped with yttrium in nacl solution. *Vestnik Magnitogorskogo Gosudarstvennogo Tekhnicheskogo Universiteta im. G.I. Vestn. Nosov Magnitogorsk State Tech. Univ.* **2016**, *14*, 95–100. [[CrossRef](#)]
- Rioja, R.J.; Liu, J. The evolution of Al-Li base products for aerospace and space applications. *Metall. Mater. Trans. A* **2012**, *43*, 3325–3337. [[CrossRef](#)]
- Li, H.; Liu, X.; Sun, Q.; Ye, L.; Zhang, X. Superplastic Deformation Mechanisms in Fine-Grained 2050 Al-Cu-Li Alloys. *Materials* **2020**, *13*, 2705. [[CrossRef](#)]
- Peng, Z.; Li, J.; Sang, F.; Chen, Y.; Zhang, X.; Zheng, Z.; Pan, Q. Structures and tensile properties of Sc-containing 1445 Al–Li alloy sheet. *J. Alloys Compd.* **2018**, *747*, 471–483. [[CrossRef](#)]
- Zhou, C.; Zhan, L.; Shen, R.; Zhao, X.; Yu, H.; Huang, M.; Li, H.; Yang, Y.; Hu, L.; Liu, D.; et al. Creep behavior and mechanical properties of Al-Li-S4 alloy at different aging temperatures. *J. Cent. South Univ.* **2020**, *27*, 1168–1175. [[CrossRef](#)]
- Li, J.F.; Liu, P.L.; Chen, Y.L.; Zhang, X.H.; Zheng, Z.Q. Microstructure and mechanical properties of Mg, Ag and Zn multi-microalloyed Al-(3.2-3.8)Cu-(1.0-1.4)Li alloys. *Trans. Nonferrous Met. Soc. China* **2015**, *25*, 2103–2112. [[CrossRef](#)]
- Gao, Z.; Chen, J.H.; Duan, S.Y.; Yang, X.B.; Wu, C.L. Complex Precipitation Sequences of Al-Cu-Li-(Mg) Alloys Characterized in Relation to Thermal Ageing Processes. *Acta Metall. Sin.* **2016**, *29*, 94–103. [[CrossRef](#)]
- Gao, C.; Luan, Y.; Yu, J.C.; Ma, Y. Effect of thermo-mechanical treatment process on microstructure and mechanical properties of 2A97 Al-Li alloy. *Trans. Nonferrous Met. Soc. China* **2014**, *24*, 2196–2202. [[CrossRef](#)]
- Sun, Y.; Aindow, M.; Hebert, R.J.; Langdon, T.G.; Lavernia, E.J. High-pressure torsion-induced phase transformations and grain refinement in Al/Ti composites. *J. Mater. Sci.* **2017**, *52*, 12170–12184. [[CrossRef](#)]
- Liu, F.; Yuan, H.; Goel, S.; Liu, Y.; Wang, J.T. Bulk nanolaminated nickel: Preparation, microstructure, mechanical property, and thermal stability. *Metall. Mater. Trans. A* **2018**, *49*, 576–594. [[CrossRef](#)]
- Wang, H.; Su, L.H.; Yu, H.L.; Lu, C.; Tieu, K.; Liu, Y.; Zhang, J. A new finite element model for multi-cycle accumulative roll bonding process and experiment verification. *Mater. Sci. Eng. A* **2018**, *726*, 93–101. [[CrossRef](#)]
- Yu, H.L.; Du, Q.L.; Godbole, A.; Lu, C.; Kong, C. Improvement in Strength and Ductility of Asymmetric-Cryorolled Copper Sheets under Low-Temperature Annealing. *Metall. Mater. Trans. A* **2018**, *49*, 4398–4403. [[CrossRef](#)]
- Yu, H.L.; Lu, C.; Tieu, K.; Li, H.J.; Godbole, A.; Kong, C.; Zhao, X. Simultaneous grain growth and grain refinement in bulk ultrafine-grained copper under tensile deformation at room temperature. *Metall. Mater. Trans. A* **2016**, *47*, 3785–3789. [[CrossRef](#)]
- Magalhães, D.C.C.; Kliauga, A.M.; Ferrante, M.; Sordi, V.L. Asymmetric cryorolling of AA6061 Al alloy: Strain distribution, texture and age hardening behavior. *Mater. Sci. Eng. A* **2018**, *736*, 53–60. [[CrossRef](#)]
- Gholinia, A.; Humphreys, F.; Prangnell, P. Processing to ultrafine grain structures by conventional routes. *Mater. Sci. Technol.* **2000**, *16*, 1251–1255. [[CrossRef](#)]
- Han, Y.; Shi, J.; Xu, L.; Cao, W.Q.; Dong, H. Effect of hot rolling temperature on grain size and precipitation hardening in a Ti-microalloyed low-carbon martensitic steel. *Mater. Sci. Eng. A* **2012**, *553*, 192–199. [[CrossRef](#)]
- Shanmugasundaram, T.; Murty, B.S.; Sarma, V.S. Development of ultrafine grained high strength Al-Cu alloy by cryorolling. *Scr. Mater.* **2006**, *54*, 2013–2017. [[CrossRef](#)]
- Deng, Y.; Huang, G.; Cao, L.; Wu, X.; Huang, L.; Xia, M.; Liu, Q. Improvement of strength and ductility of Al–Cu–Li alloy through cryogenic rolling followed by aging. *Trans. Nonferrous Met. Soc. China* **2017**, *27*, 1920–1927. [[CrossRef](#)]
- Li, C.; Xiong, H.Q.; Bhatta, L.; Wang, L.; Zhang, Z.Y.; Wang, H.; Kong, C.; Yu, H.L. Microstructure evolution and mechanical properties of Al–3.6Cu–1Li alloy via cryorolling and aging. *Trans. Nonferrous Met. Soc. China* **2020**, *30*, 2904–2914. [[CrossRef](#)]
- Saimoto, S. Deformation kinetics and constitutive relation analyses of bifurcation in work-hardening of face-centred cubic metals at cryogenic temperatures. *Acta Mater.* **2019**, *174*, 43–52. [[CrossRef](#)]

23. Jayaganthan, R.; Panigrahi, S.K. Effect of Cryorolling Strain on Precipitation Kinetics of Al 7075 Alloy. *Mater. Sci. Forum* **2008**, *584–586*, 911–916. [[CrossRef](#)]
24. Tanaka, Y.; Masumura, T.; Tsuchiyama, T.; Takaki, S. Effect of dislocation distribution on the yield stress in ferritic steel under identical dislocation density conditions. *Scr. Mater.* **2020**, *177*, 176–180. [[CrossRef](#)]
25. Ma, K.; Wen, H.; Hu, T.; Topping, T.; Isheim, D.; Seidman, D.; Lavernia, E.; Schoenung, J. Mechanical behavior and strengthening mechanisms in ultrafine grain precipitation-strengthened aluminum alloy. *Acta Mater.* **2014**, *62*, 141–155. [[CrossRef](#)]
26. Ma, Y.; Zhou, X.; Thompson, G.E.; Hashimoto, T.; Thomson, P.; Fowles, M. Distribution of intermetallics in an AA 2099-T8 aluminium alloy extrusion. *Mater. Chem. Phys.* **2011**, *126*, 46–53. [[CrossRef](#)]
27. Pathak, M.K.; Joshi, A.; Mer, K.K.S.; Jayaganthan, R. Mechanical properties and microstructural evolution of bulk UFG Al 2014 processed through cryorolling and warm rolling. *Acta Metall. Sin.* **2019**, *32*, 845–856. [[CrossRef](#)]
28. Kumar, P.; Singh, A. Investigation of fracture behaviour and low cycle fatigue properties of cryorolled Al-Mg alloy. *Theor. Appl. Fract. Mech.* **2018**, *98*, 78–94. [[CrossRef](#)]
29. Fu, B.; Fu, L.; Liu, S.; Wang, H.R.; Wang, W.; Shan, A. High strength-ductility nano-structured high manganese steel produced by cryogenic asymmetry-rolling. *J. Mater. Sci. Technol.* **2018**, *34*, 695–699. [[CrossRef](#)]
30. Li, R.; Zhang, S.; Kang, H.; Chen, Z.; Yang, F.; Wang, W.; Zou, C.; Li, T.; Wang, T. Microstructure and texture evolution in the cryorolled CuZr alloy. *J. Alloys Compd.* **2017**, *693*, 592–600. [[CrossRef](#)]